Catalysis Today 158 (2010) 114–120

Contents lists available at ScienceDirect

Catalysis Today

journal homepage: www.elsevier.com/locate/cattod

Relevance of the physicochemical properties of CaO catalysts for the methanolysis of triglycerides to obtain biodiesel

D. Martín Alonso[a], F. Vila[a], R. Mariscal[a,*], M. Ojeda[a], M. López Granados[a], J. Santamaría-González[b]

[a] Instituto de Catálisis y Petroleoquímica (CSIC), C/Marie Curie 2, Campus de Cantoblanco, 28049 Madrid, Spain
[b] Departamento de Química Inorgánica, Cristalografía y Mineralogía (Unidad Asociada al ICP-CSIC), Facultad de Ciencias, Universidad de Málaga, Campus de Teatinos, 29071 Málaga, Spain

ARTICLE INFO

Article history:
Available online 11 June 2010

Keywords:
Biodiesel
Transesterification
CaO catalysts
Surface basicity
Pyrrole

ABSTRACT

A series of CaO solids have been prepared by means of thermal treatment of the following precursors: carbonate, acetate, oxalate, nitrate, and two hydroxides obtained previously by precipitation of calcium acetate and nitrate in basic medium. These solids show distinct reaction rates in the catalytic transesterification of triglycerides with methanol to obtain biodiesel. An exhaustive characterization study using X-ray diffraction, N_2 adsorption–desorption isotherms, infrared spectroscopy of pyrrole adsorbed, and temperature-programmed desorption of CO_2 allowed us to determine the influence of the physicochemical properties (crystallite size, surface area and porosity) and surface basicity (amount and distribution of basic sites with different strength) on the overall catalytic activity. We have found that CaO obtained by decomposition of calcium carbonate, which shows the highest amount and surface density of very strong base sites, catalyzes triglycerides transesterification with higher rates.

1. Introduction

Biodiesel, a mixture of fatty acid methyl esters (FAME), is produced from vegetable oils by transesterification of triglycerides with methanol. It is therefore an environmentally friendly and renewable fuel arising from biomass that can replace conventional diesel [1,2]. Current technology to produce biodiesel involves homogeneous base catalysis, typically NaOH or KOH dissolved in corrosive methanol is used as catalysts. This process presents, however, important limitations for competitive industrial production. Specifically, the cost of biodiesel manufacture is relatively high when compared to that of conventional diesel. Moreover, the recovery of the catalyst used in the homogeneously catalyzed industrial process is a complex and expensive step. Consequently, the effluent streams must be neutralized with an acid and separated from the methyl ester phase at the end of the reaction, with the concomitant generation of a large volume of wastewater [1,3].

The use of a successful solid catalyst will cope with the economical and environmental issues of the homogeneous process. In particular, this would result in some relevant improvements of biodiesel production, such as reusability of the catalyst, ease separation of the reaction products and catalyst by filtration, and facile separation and purification of the biodiesel and glycerol phases, thus decreasing significantly the amount of water required to wash the reaction products [4–6]. These benefits associated with the use of solid catalysts for biodiesel production have promoted to intensive scientific research in this field.

Solid basic catalysts, as MgO, ZnO, CeO_2 and La_2O_3, have been tested in the transesterification reaction of triglycerides with methanol to obtain biodiesel. It was found that those solids with a higher basicity catalyze the transesterification reaction more efficiently [7]. Bulk CaO has been recently identified as a promising active and reusable catalyst for this transesterification reaction [8–11]. Previous works have concluded that particle size and activation process influence significantly its catalytic behavior. The basic character shown by CaO can be increased by adding an alkaline metal [12,13] or by submerging the solid into an ammonium carbonate solution [14].

The route used to prepare different metal oxides is a critical aspect that determines the physicochemical properties of the resulting solids [15]. In particular, the preparation protocol of alkaline earth oxides affects significantly the resulting surface area. Indeed, several authors have studied the textural properties of MgO obtained by decomposition of several precursor salts and hydroxides [16,17], finding that higher surface area values were obtained when using magnesium oxalate as a precursor because the gases evolved during the thermal treatment required to form MgO generate a more porous structure. In contrast, MgO solids displaying low surface area were obtained when $MgCl_2$ was employed as a precursor because chlorine ions provoke the agglomeration of the MgO crystallites. Similar trends were also observed with respect to the base character shown by MgO. On the other hand, alkaline

* Corresponding author. Tel.: +34 91 5854938; fax: +34 91 5854760.
E-mail address: r.mariscal@icp.csic.es (R. Mariscal).

0920-5861/$ – see front matter © 2010 Elsevier B.V. All rights reserved.
doi:10.1016/j.cattod.2010.05.003

earth metal oxides (CaO) have been recently reported as promising solid catalysts in the glycerol etherification reaction [18,19]. These authors prepared different CaO materials and found that these solids display distinct surface area values, number of basic sites and surface topology, which were relevant in glycerol etherification.

In this context, we have performed a detailed and rigorous study of the preparation route of CaO and starting precursors to establish the importance of these two parameters on the physicochemical properties and the catalytic activity in transesterification reactions. The experimental approach has consisted in the preparation of a series of CaO solids by thermal decomposition of different precursors, carbonate, acetate, oxalate, nitrate, and two hydroxides obtained by precipitation of calcium acetate and calcium nitrate solutions. Their activities in the methanolysis of the commercial sunflower oil to produce biodiesel were evaluated under mild conditions (atmospheric pressure and 323 K) and in order to explain the observed catalytic behavior, samples were characterized by evolving gas analysis by mass spectrometry, X-ray diffraction, N_2 adsorption–desorption isotherms, infrared spectroscopy of pyrrole adsorbed, and temperature-programmed desorption of CO_2.

2. Experimental

2.1. Preparation of catalysts

Four calcium oxide samples were prepared by thermal decomposition of commercially available calcium salts: calcium carbonate ($CaCO_3$, Sigma–Aldrich, A.C.S. Reagent), calcium acetate hydrate ($Ca(CH_3COO)_2{\cdot}xH_2O$, Sigma–Aldrich, >99%), calcium oxalate hydrate ($CaC_2O_4{\cdot}xH_2O$, Aldrich), and calcium nitrate tetrahydrate ($Ca(NO_3)_2{\cdot}4H_2O$, Sigma–Aldrich, >99%). These decomposed samples were labelled as CaO–C, CaO–A, CaO–O, and CaO–N respectively. Two additional samples were obtained by decomposition of $Ca(OH)_2$ previously prepared by precipitation from aqueous solutions (1 M) of calcium acetate and calcium nitrate salts by adding slowly an excess (1.2 times) of the theoretical amount of a NaOH solution (2 M) required to precipitate all Ca^{2+} as $Ca(OH)_2$. N_2 was continuously passed through the solution to prevent the carbonation of the precipitated $Ca(OH)_2$. The solids were recovered by filtration under N_2, then dried overnight at room temperature under nitrogen flow and finally, treated at high temperature in O_2/Ar mixtures (details are given later). These samples were labelled as CaO/OH–A (from acetate) and CaO/OH–N (from nitrate). Chemical analysis of these two hydroxides revealed the absence of Na impurities.

2.2. Activity measurements

The transesterification reaction of commercial food-grade sunflower oil was carried out in a 100-mL jacketed three-necked glass reactor with a condenser and a dropping funnel. Precursors were decomposed under a 20 vol.% O_2/Ar flow (40 mL min^{-1}) at 1073 K (heating rate of 10 K min^{-1}) for 1 h to yield *ca.* 100 mg of CaO. The solid was then contacted with anhydrous methanol (27 g, Riedel-de Häen, 99.8%) while avoiding exposure to ambient air. More details about the experimental procedures have been described elsewhere [20]. Subsequently, the temperature of the methanol–solid mixture was raised to 323 K under N_2. The reaction was started when preheated sunflower oil (50 g) at 323 K was added to the reactor through the dropping funnel. This three-phase system was vigorously stirred (1000 rpm). The reaction was conducted at atmospheric pressure for 3 h.

Aliquots were periodically extracted with a syringe for sampling analysis, neutralized with a 0.1 M HCl solution to prevent the reaction to continue, and then washed with dichloromethane. The alcoholic phase (water, glycerine and methanol in excess) was separated from the organic phase (dichloromethane and fatty acid methyl esters) by decantation. Residual dichloromethane in the methyl ester phase was removed by evaporation. After purification of the methyl esters phase, quantitative analysis was carried out according to the European normative EN-14103. Further information about biodiesel analysis can be found elsewhere [10,13].

2.3. Characterization techniques

Evolved gas analysis at programmed temperature by mass spectrometry (EGA-MS) was performed by loading the precursors (*ca.* 100 mg) in a U-shaped quartz microreactor and treating the solid with a 20 vol.% O_2/Ar flow (80 mL min^{-1}) while heating at 10 K min^{-1} until 1073 K. In the case of the calcium acetate experiment, the solid (50 mg) was diluted with SiC (50 mg) and treated with a 5 vol.% O_2/Ar flow (80 mL min^{-1}) because the decomposition reaction is highly exothermic. A quadruple mass spectrometer (BALZERS Prisma QMS 200) controlled by BALTZER Quadstar™ 422 software was connected on-line to the reactor outlet for the analysis of H_2O (m/z = 18), NO (m/z = 30), O_2 (m/z = 32), Ar (m/z = 40), and CO_2 (m/z = 44).

Powder X-ray diffraction (XRD) patterns were recorded at room temperature in the 20–80° range in the scan mode (0.02°, 1 s) with a Siemens D5000 automated diffractometer over a 2θ Bragg–Brentano geometry, using Cu Kα radiation and a graphite monochromator. Samples were previously activated *in situ* at 1073 K for 1 h under a 20 vol.% O_2/Ar flow.

Nitrogen adsorption–desorption isotherms were recorded at the temperature of liquid nitrogen (77 K) using a Micromeritics ASAP 2000 apparatus. Samples were previously degassed under activation conditions, a 20 vol.% O_2/Ar flow (40 mL min^{-1}) at 1073 K (heating rate of 10 K min^{-1}).

Pyrrole (C_4H_4NH) has been previously used as a probe molecule of base solids because of its amphoteric character [21,22]. Thus, the basicity of the CaO catalysts was evaluated by Fourier transform infrared (FTIR) spectroscopy of adsorbed pyrrole. The spectra were recorded with a Nicolet 5700 spectrometer equipped with a globar source and an Hg–Te–Cd type cryodetector. The spectra reported here are the average of 256 scans at 4 cm^{-1} resolution and plotted in the absorbance mode. Experimentally, the CaO solids were pressed into self-supporting wafers (*ca.* 10 mg cm^{-2}), placed in a sample holder, degassed at 1073 K for 1 h ($<5 \times 10^{-4}$ Torr) and then cooled down to room temperature. Subsequently, pyrrole *ca.* 2 Torr (1 Torr = 133.3 N m^{-2}) was dosed into the cell during 15 min. The fraction of physically adsorbed pyrrole was removed by degassing at room temperature for 30 min. Prior to the adsorption of pyrrole, a background spectrum of the solid was recorded. The FTIR spectra were obtained after subtracting the background spectrum.

Temperature-programmed desorption of CO_2 (TPD–CO_2) was carried out in the U-reactor connected to a mass spectrometer described above. The catalytic precursors (*ca.* 175 mg) were treated in synthetic air (40 mL min^{-1}) at 1073 K (ramp of 10 K min^{-1}) for 1 h. The samples were then cooled down to room temperature. Afterwards, CO_2 adsorption was performed by passing a 23 vol.% CO_2/Ar flow (20 mL min^{-1}) for 1 min. This procedure saturates slightly the CaO surface with CO_2 considering the surface oxygen density (O-atoms nm^{-2}) estimated for the most stable (0 0 1) plane of CaO [23], but impedes the formation of bulk calcium carbonate. Finally, the CO_2-containing flow was switched to Ar (50 mL min^{-1}) and the solid was heated at 10 K min^{-1} until 1073 K. The CO_2 signal was previously calibrated by dosing different CO_2 pulses in an empty reactor to quantify the amount of CO_2 chemisorbed on the surface.

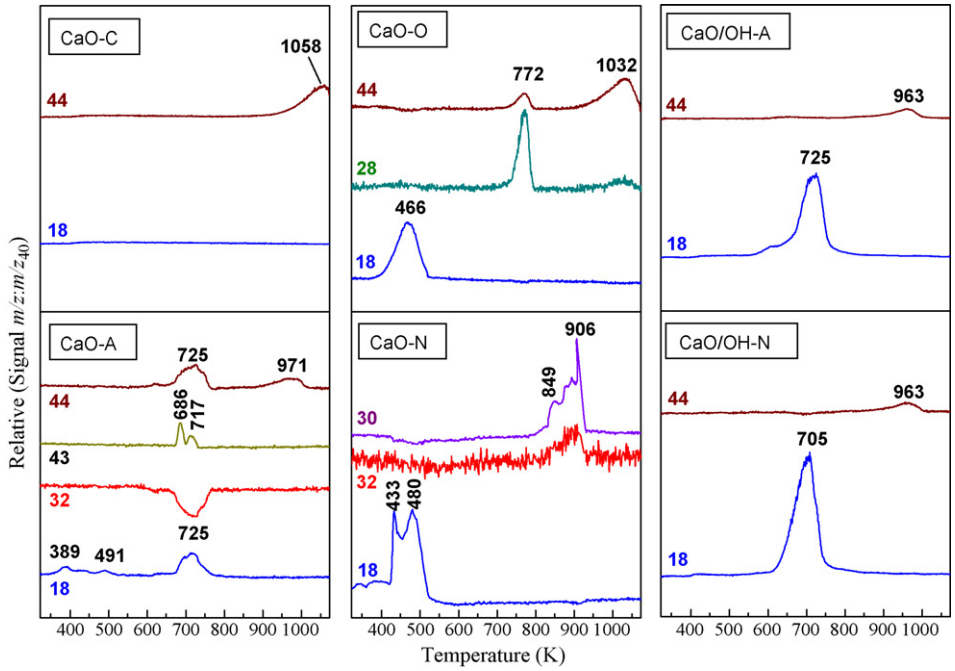

Fig. 1. EGA-MS profiles obtained during the decomposition calcium carbonate (CaO–C), calcium acetate (CaO–A), calcium oxalate (CaO–O), calcium nitrate (CaO–N), and calcium hydroxide formed via precipitation of calcium acetate (CaO/OH–A) or calcium nitrate (CaO/OH–N). Fragments m/z = 18, 28, 30, 32, 43 and 44 stand for H_2O^+, CO^+, NO^+, O_2^+, $C_2H_3O^+$, and CO_2^+, respectively.

3. Results and discussion

3.1. Activation process and catalytic behavior of CaO

$Ca(OH)_2$ and $CaCO_3$ are not active catalysts for the transesterification reaction of triglycerides with methanol. Hence, it is necessary to treat these precursors at high temperature to obtain CaO, which is known to efficiently catalyze the transesterification reaction that form biodiesel [10,24].

The temperature required to transform the different catalytic precursors (calcium carbonate, calcium acetate, calcium oxalate, calcium nitrate, and two calcium hydroxides obtained by acetate and nitrate solution precipitation respectively with NaOH) into CaO was obtained from the EGA-MS experiments (Fig. 1). Calcium carbonate ($CaCO_3$) yields calcium oxide (CaO–C) via a decarbonation step (Eq. (1)) with a maximum decomposition rate at 1058 K:

$$CaCO_3 \rightarrow CaO + CO_2 \quad (1)$$

In contrast, calcium acetate ($Ca(C_2H_3O_2)_2{\cdot}xH_2O$) decomposes into calcium oxide (CaO–A) in two consecutive steps. First, the organic anion is combusted (oxygen consumption) at 650–775 K to give $CaCO_3$, H_2O and CO_2:

$$Ca(C_2H_3O_2)_2 + 4O_2 \rightarrow CaCO_3 + 3H_2O + 3CO_2 \quad (2)$$

The calcium carbonate formed in this step decomposes subsequently at 900–1000 K to give CaO and CO_2 according to Eq. (1). Fragments corresponding to CH_3CO^+ (m/z = 43) and CH_3^+ (m/z = 15; not shown) were detected at 686–717 K, while desorption of hydration water occurs at <500 K.

Calcium oxalate ($CaC_2O_4{\cdot}xH_2O$) also forms calcium oxide (CaO–O) in two successive steps. Thus, a decarbonation process with a maximum rate at 772 K occurs first. We have observed an intense peak corresponding to CO^+ fragments (m/z = 28), indicating that the oxalate decomposes into CO and CO_2:

$$CaC_2O_4 + O_2 \rightarrow CaCO_3 + CO_2, CO \quad (3)$$

Again, the calcium carbonate decomposes afterwards to CaO and CO_2 at 1000–1040 K. Desorption of hydration water is observed at temperatures between 400 and 525 K.

Calcium nitrate tetrahydrate ($Ca(NO_3)_2{\cdot}4H_2O$) decomposes at 800–910 K (maximum rate at 906 K) in a single step to give calcium oxide (CaO–N), NO and O_2:

$$Ca(NO_3)_2 \rightarrow CaO + 2NO + (3/2)O_2 \quad (4)$$

Different hydration water removal steps are also observed at temperatures below 550 K.

Finally, both calcium hydroxides show an intense water formation peak at 705–725 K assigned to their decomposition

$$Ca(OH)_2 \rightarrow CaO + H_2O \quad (5)$$

Minor peaks corresponding to CO_2 desorption are also detected at 963 K in these profiles, which can be related to ambient CO_2 previously adsorbed on the solid surface.

Summarizing EGA-MS results, we have found that the generation of CaO from calcium acetate and calcium oxalate occurs at 900–1050 K via $CaCO_3$ species previously formed. In contrast, the $Ca(NO_3)_2$ precursor decomposes at 800–900 K directly to CaO. The two calcium hydroxides form CaO at 705–725 K. For the sake of comparison, we have treated all the CaO precursors in synthetic air at 1073 K for 1 h to thus guarantee their complete decomposition and formation of pure CaO. The solids were then cooled down in N_2 flow and loaded into the batch reactor while avoiding any contact with ambient air to prevent sample hydration and carbonation before measuring their catalytic activity [20].

Fig. 2 presents the rate of FAME formation (mol h^{-1} g_{cat}^{-1}) measured with the different CaO catalysts, which can be divided into two groups. The first one, constituted by CaO–C, CaO–A, CaO–O and CaO/OH–A, are active catalysts for triglycerides transesterification with minor differences among them, reaching FAME yields close to 90% after 3 h of reaction. The second group, CaO/OH–N and CaO–N, are almost inactive in the transesterification reaction. We note here that irrespective of the exact identity of the precursor used, those formed from nitrate compounds are much less active than the

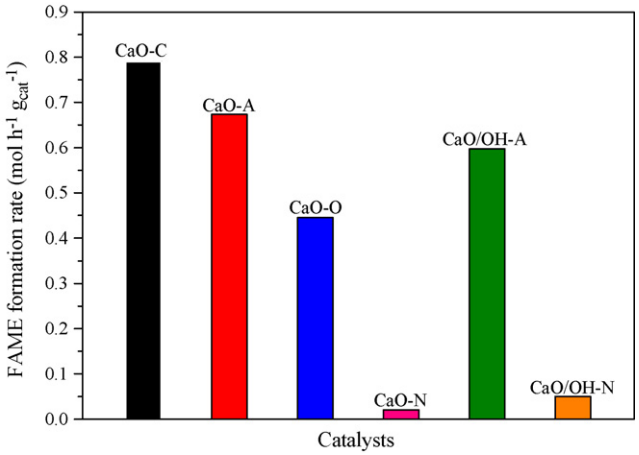

Fig. 2. Rate of FAME formation measured with the CaO catalysts after 1 h in reaction.

others. This is especially evident upon comparing the catalytic activity shown by the two CaO solids formed via $Ca(OH)_2$ derived from acetate (active) and nitrate (inactive). A detailed and rigorous characterization study of all CaO samples has been then carried out to identify the reasons of the different catalytic behaviors.

3.2. Structural characterization of CaO catalysts

Fig. 3 collects the XRD patterns of the CaO samples activated *in situ* under synthetic air flow at 1073 K for 1 h. Irrespective of the identity of the starting precursors used, all the samples show the diffraction lines attributed to the presence of crystalline CaO (JCPDS 77-2376) after the activation process. All the diffractograms have been normalized to the reflection (2 0 0). Therefore, our data suggest that the differences observed in activity cannot be attributed to an incomplete decomposition of the precursors during the activation step, because diffraction peaks other than those assigned to CaO are not observed. These results are essentially consistent with recent reports showing XRD patterns for CaO solids obtained upon treating different precursors in N_2 at high temperature [25]. Crystal size data for CaO samples calculated from the Debye–Scherrer equation using the CaO reflection (2 0 0) at $2\theta = 37.4^\circ$ are depicted in Table 1. Certain agglomeration of individual particles may occur during the *in situ* activation process, although this should not affect the accuracy of the crystal size determined by XRD.

Significant variations (from 37 to 116 nm) are detected as a function of the CaO precursor. The smallest CaO particles are formed with calcium acetate and calcium oxalate precursors. In contrast, much larger particles are originated when calcium nitrate is used as precursor (CaO–N and CaO/OH–N).

3.3. Textural characterization of CaO catalysts

Table 1 shows BET surface area and pore size values measured for the different CaO solids. We note that those catalysts that

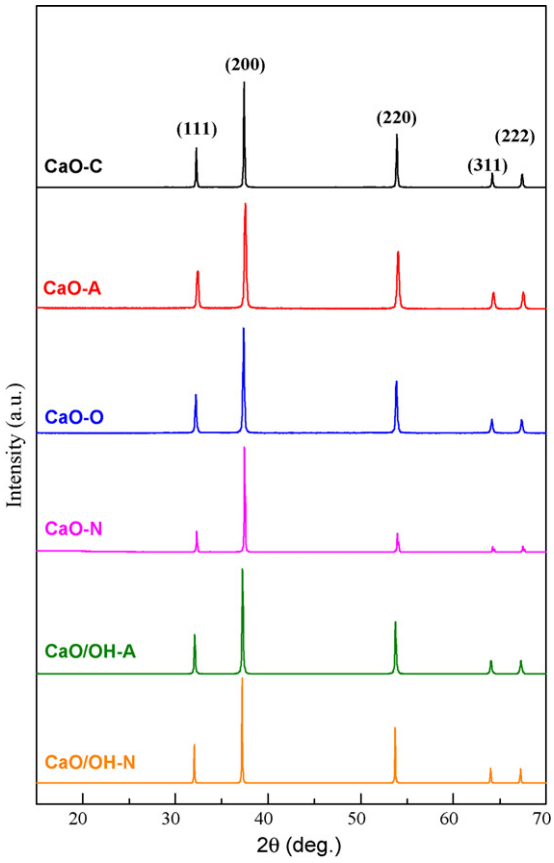

Fig. 3. X-ray diffraction patterns of CaO solids after treating the different precursors in synthetic air at 1073 K for 1 h.

show high transesterification rates, that is, CaO samples obtained from calcium carbonate, acetate, oxalate and hydroxide from precipitation of calcium acetate solution, display surface area values ranging from 22 to 27 $m^2\ g^{-1}$. In contrast, those CaO samples prepared from nitrate precursors show low surface areas (<7 $m^2\ g^{-1}$), which results in catalysts with low transesterification reaction rates. Our data confirm, therefore, the relevance of the surface area, and in lower extent the crystallites size, in obtaining active CaO catalysts.

The CaO samples prepared from nitrate precursors show low surface areas, large crystallites, and consequently, low reaction rates. It is known that calcium nitrate melts during the activation process before decomposes, and some authors have attributed to this phenomenon its low surface area and poor catalytic performance [26]. However, we note that this explanation alone does not justify the low activity measured with the CaO/OH–N catalyst. In this case, the low surface BET area displayed may be associated with the presence of occluded nitrate ions in the structure of the catalytic precursor [16].

Table 1
Structural and textural properties of CaO catalysts.

Sample	Crystal size[a] (nm)	Surface area ($m^2\ g^{-1}$)	Pore volume ($cm^3\ g^{-1}$)	Pore diameter (nm)
CaO–C	67	26	0.27	41
CaO–A	37	22	0.18	33
CaO–O	47	26	0.24	38
CaO–N	116	<1	–	–
CaO/OH–A	60	27	0.16	24
CaO/OH–N	93	7	0.05	33

[a] Estimated from XRD line width of main reflection at 37.4° (2 0 0)

3.4. Characterization of surface basicity of CaO

Carbon dioxide is typically used as a probe molecule for the characterization of the surface basicity of solids. Therefore, we performed preliminary FTIR experiments of CO_2 adsorption over the CaO samples to determine the identity and strength of surface base sites. We observed a broad band in the carbonate region of the infrared spectrum (1600–1300 cm^{-1}) that unfortunately, did not allow us to extract reliable information. Consequently, we have selected pyrrole (C_4H_4NH; denoted here as PYH) as a probe molecule to measure the basicity of CaO because of its weak acidity ($pK_a \approx 15$). Although the use of pyrrole increases the complexity of the interpretation and assignments of the infrared bands because that molecule can interact with both acid and base sites, the interaction with these latter sites is well documented in the literature [21,22,27–29]. Pyrrole can interact with surface basic sites via either dissociative or non-dissociative adsorption, depending on the strength of the sites. Thus, pyrrole can be adsorbed molecularly onto the base framework oxygen atoms (O^{2-}) and/or OH^- sites. This formation results in the shifting of the broad band due to N–H stretching centered at 3497 cm^{-1} (measured in CCl_4) to lower frequencies. Moreover, the absolute value of the shifting increases with the strength of the base sites. Alternatively, pyrrole can be also adsorbed dissociatively to give pyrrolate anions. This occurs with very strong basic metal oxides, where deprotonation of pyrrole on the strongest basic sites leads to the production of pyrrolate anions (PY^-) stabilized by surface cations or by acid sites. The formation of these pyrrolate anions causes the downshifting of the ring vibrational stretching frequency from 1522 for pyrrole to *ca.* 1452 cm^{-1} for pyrrolate anions. In addition, the dissociative adsorption of pyrrole causes a decrease in the frequency of the C–H stretching vibration, ν(CH), as well as the appearance of two bands at 3100 and 3050 cm^{-1}. The π-electrons of the pyrrole molecule also act as an H-acceptor when interacting with hydroxyl groups. The formation of a H-bond between the surface hydroxyl groups and pyrrole provokes the decrease of the OH stretching bands to lower frequencies [27,28].

Based on these arguments, we can assign the main features observed in the infrared spectra of pyrrole adsorbed on the more representative activated CaO catalysts (Fig. 4). For the sake of clarity, the spectra are shown in two regions: 3800–2800 cm^{-1} and 1500–1400 cm^{-1}. We observe a broad band at 3700–3200 cm^{-1}, in which the peak centered at 3589 cm^{-1} is assigned to hydroxyl groups perturbed by the interaction with pyrrole [29,30]. Our attention is focused, however, on the broad band related to the N–H stretching vibration, which presents two maxima at around 3450 and 3320 cm^{-1}. This broad band, associated with the non-dissociative interaction of pyrrole with basic sites [21,22,27] is detected with all our CaO catalysts. Furthermore, three sharp bands at 3093, 3052 and 2956 cm^{-1} are also present. The first two bands are associated with ν(C–H) stretching vibrations, while the latter is attributed to a combination band, which are indicative of the presence of strong basic sites [21,27,28]. This is confirmed by the presence of a band centered at 1446 cm^{-1} due to ν(C=C) stretching ring vibrations, also indicative of the formation of pyrrolate anions.

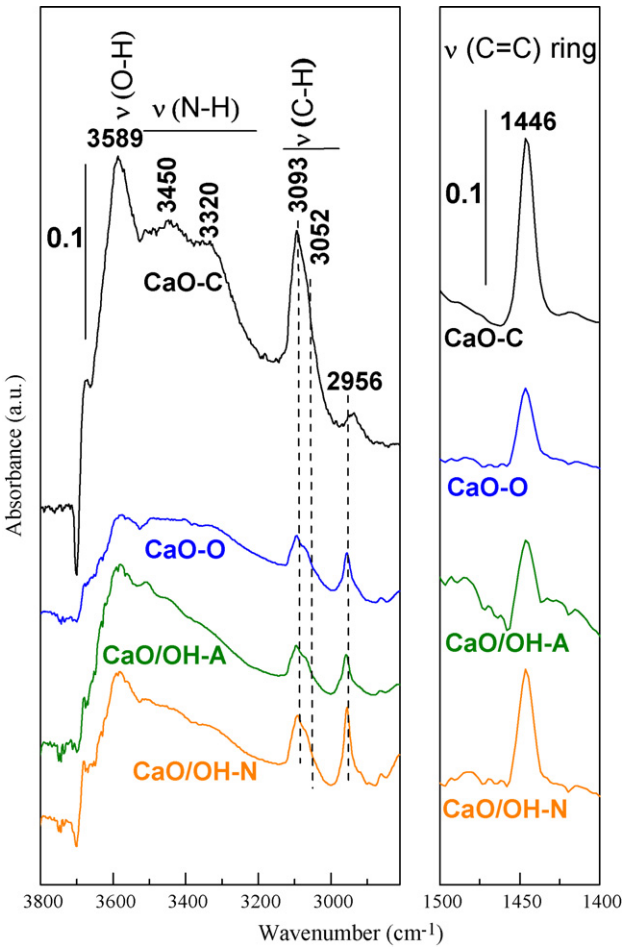

Fig. 4. FTIR spectra of pyrrole adsorbed (2 Torr) on the different CaO catalysts.

The thermal stability of the infrared bands was studied upon degassing the samples for 30 min at increasing temperatures (323, 373 and 423 K) and then cooling down to room temperature (spectra not shown for the sake of clarity). In all cases, the intensity of the IR bands decreased upon increasing the degassing temperature, but no significant differences were observed among the different catalysts.

Based on the FTIR results of pyrrole adsorption on CaO, we conclude that two types of basic sites are present in these solids: (i) strong basic sites that adsorb pyrrole molecularly (identified by the N–H stretching vibrations) and (ii) very strong basic sites, which adsorb pyrrole dissociatively to form pyrrolate anions. Since it is not possible to determine quantitatively the distribution of each type of base sites with the FTIR experiments, we have obtained these numbers from temperature-programmed desorption of CO_2 (TPD–CO_2) following protocols similar to those described in the literature for other metal oxide solids [31–34].

Table 2
Amount of CO_2 desorbed (from TPD experiments) normalized by mass of solid (μmol g^{-1}) or specific surface area (μmol m^{-2}).

Sample	CO_2 desorbed (μmol g^{-1})			Total CO_2 desorbed (μmol m^{-2})
	At 815 K	At 878 K	Total	
CaO–C	48	53	101	3.9
CaO–A	43	19	62	2.8
CaO–O	36	27	63	2.4
CaO–N	–	–	–	–
CaO/OH–A	18	43	61	2.3
CaO/OH–N	5	10	15	2.2

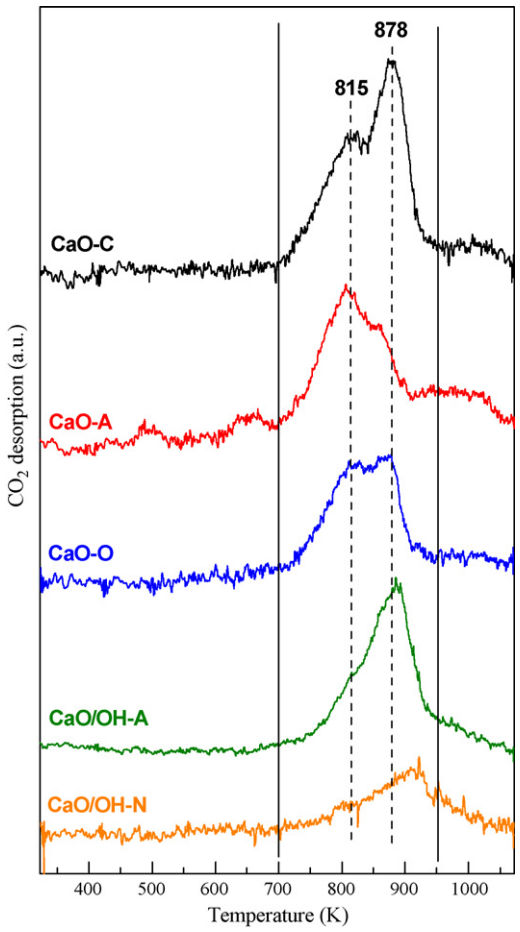

Fig. 5. TPD–CO_2 profiles of the activated CaO catalysts.

Fig. 5 depicts the TPD–CO_2 profiles where signals are normalized by catalyst mass. As described previously, FTIR of adsorbed pyrrole experiments revealed the presence of strong (adsorb pyrrole molecularly) and very strong base sites (adsorb pyrrole dissociatively). Consistent with these results, all the TPD profiles display two desorption peaks at 815 and 878 K that correspond to CO_2 desorption from the strong and very strong base sites, respectively. Table 2 compiles the individual and total amounts of CO_2 desorbed (values obtained by integrating in the range 700–950 K in TPD–CO_2 profiles) normalized by mass of solid and specific surface area. We have not found any relationship between the measured rates of triglycerides transesterification with methanol and the relative concentration of the two types of base sites. This is somewhat expected because both sites identified on CaO samples possess similar basic strength, which may be sufficiently strong to catalyze the transesterification reaction. Instead, the activity shown for the different CaO samples seems to be related to the total amount of CO_2 desorbed in each case, that is, with the overall number of base sites. Indeed, CaO–C shows both the highest ability to adsorb CO_2 (indicative of a higher number of base sites) and the highest reaction rates, whereas CaO–N, which is almost inactive in the transesterification reaction, does not adsorb measurable amounts of CO_2. In conclusion, it seems that the activity of samples depends on the overall amount of basic sites instead of their relative concentration, which indicates that both types of base sites are active in the transesterification reaction.

Concerning to the nature of the basic sites (O^{2-} and OH species) present on the solid surface, we would like to mention that working at extremely low H_2O partial pressures ($\leq 5 \times 10^{-9}$ Torr) is required to prevent the hydration of the surface top layers of CaO to yield surface $Ca(OH)_2$ at room temperature [10,35,36]. The calcium hydroxide species are formed via reaction of strong basic lattice oxygen of CaO with atmospheric moisture. The very low water concentrations can be only achieved with appropriate ultra high vacuum (UHV) equipments, which means that in practical terms and under conditions frequently faced in common experimentation, $Ca(OH)_2$ is inevitably present on the solid surface. Consequently, the two types of basic sites detected by FTIR after adsorption of pyrrole and TPD–CO_2 should be associated with hydroxyl groups placed in surface sites with different coordination (terraces or steps), although some effect of the sub-surface O^{2-} on the basicity strength cannot be completely discarded.

3.5. Structure–activity relationships

The identity of the calcium salt used to prepare CaO by thermal decomposition has shown to have a significant influence in its physicochemical properties. Comparing the rates of sunflower oil transesterification displayed by the different CaO solids (Fig. 2) with their physicochemical characterization results, we find a straightforward relationship between surface basicity (directly related to the surface area) and the catalytic activity. Although this may be rather expected, we would like to remark that for the first time, the surface density of base sites (a combination of surface area and overall number of base sites) is highlighted as a relevant parameter to explain the catalytic behavior in transesterification reactions when different CaO solids show similar numbers of strong and very strong base sites.

When calcium nitrate is used as a CaO precursor, the resulting solids show large crystallites and a small number of base sites (due to the resulting low surface area), irrespective of the methodology selected for the preparation, direct decomposition at high temperature or previous formation of $Ca(OH)_2$ by precipitation in basic medium and subsequent decomposition. Two types of base sites have been identified in these activated CaO catalysts: (i) strong base sites (detected from the IR band associated with the N–H stretching of pyrrole adsorbed, and from the peak observed in the TPD–CO_2 profiles at 815 K) and (ii) very strong base sites (pyrrolate formation in FTIR spectra and TPD–CO_2 peak at 878 K). Both sites are catalytically active in the transesterification reaction of triglycerides with methanol at mild conditions. Therefore, we conclude that future investigations should focus on the preparation of CaO solids with high surface areas and large number of strong/very strong base sites, which would be reflected in high transesterification rates.

4. Conclusions

Calcium oxide obtained by decomposition of carbonate precursor has shown to be the most active catalyst in the transesterification reaction of triglycerides with methanol to obtain biodiesel. In contrast, CaO obtained via decomposition of nitrate precursors showed the lowest reaction rates. The catalytic performance of calcium oxide samples is determined by the total amount of surface base sites and/or surface area values. For those CaO samples showing similar numbers of strong base sites, the surface density of these basic sites is the key parameter to explain the measured reaction rates.

Acknowledgements

Financial support from the Spanish Ministry of Science and Innovation (ENE2006-15116-C04-01/CON) is gratefully acknowledged. M.O thanks CSIC for financial support through the JAE-Doc program.

References

[1] F. Ma, M.A. Hanna, Bioresour. Technol. 70 (1999) 1.
[2] A. Srivastava, R. Prasad, Renew Sust. Energy Rev. 4 (2000) 111.
[3] J. van Gerpen, Fuel Process. Technol. 86 (2005) 1097.
[4] M. Di Serio, R. Tesser, L. Pengmei, E. Santacesaria, Energy Fuels 22 (2008) 207.
[5] J. van Gerpen, R. Pruszko, D. Clements, B. Shanks, G. Knothe, Building a Successful Biodiesel Business, second ed., Biodiesel Basics, 2006.
[6] G. Knothe, J. van Gerpen, J. Krahl, The Biodiesel Handbook, AOCS Press, 2005.
[7] S. Bancquart, C. Vanhove, Y. Pouilloux, J. Barrault, Appl. Catal. A: Gen. 218 (2001) 1.
[8] S. Gryglewicz, Bioresour. Technol. 70 (1999) 249.
[9] X. Liu, X. Piao, Y. Wang, S. Zhu, H. He, Fuel 87 (2008) 1076.
[10] M. López Granados, M.D.Z. Poves, D. Martin Alonso, R. Mariscal, F. Cabello Galisteo, R. Moreno-Tost, J. Santamaria, J.L.G. Fierro, Appl. Catal. B: Environ. 73 (2007) 317.
[11] C. Reddy, V. Reddy, R. Oshel, J.G. Verkade, Energy Fuels 20 (2006) 1310.
[12] R.S. Watkins, A.F. Lee, K. Wilson, Green Chem. 6 (2004) 335.
[13] D.M. Alonso, R. Mariscal, M.L. Granados, P. Maireles-Torres, Catal. Today 143 (2009) 167.
[14] H.P. Zhu, Z.B. Wu, Y.X. Chen, P. Zhang, S.J. Duan, X.H. Liu, Z.Q. Mao, Chin. J. Catal. 27 (2006) 391.
[15] K. Zhu, J. Hu, C. Kübel, R. Richards, Angew Chem. Int. Ed. 45 (2006) 7277.
[16] V.R. Choudhary, M.Y. Pandit, Appl. Catal. 71 (1991) 265.
[17] T. Matsuda, J. Tanabe, N. Hayashi, Y. Sasaki, H. Miura, K. Sugiyama, Bull. Chem. Soc. Jpn. 55 (1982) 990.
[18] A.M. Ruppert, J.D. Meeldijk, B.W.M. Kuipers, B.H. Erné, B.M. Weckhuysen, Chem. Eur. J. 14 (2008) 2016.
[19] M. Calatayud, A.M. Ruppert, B.M. Weckhuysen, Chem. Eur. J. 15 (2009) 10864.
[20] M. López Granados, D. Martín Alonso, A.C. Alba-Rubio, R. Mariscal, M. Ojeda, P. Brettes, Energy Fuels 23 (2009) 2259.
[21] D. Murphy, P. Massiani, R. Franck, D. Barthomeuf, J. Phys. Chem. 100 (1996) 6731.
[22] J. Kucera, P. Nachtigall, J. Kotrla, G. Kosová, J. Cejka, J. Phys. Chem. B 108 (2004) 16012.
[23] M. Calatayud, Ethylene glycol interaction on alkaline earth oxides: a periodic DFT study, Catal. Today (2009), doi:10.1016/j.cattod.2009.08.11.
[24] M. Kouzu, T. Kasuno, M. Tajika, Y. Sugimoto, S. Yamanaka, J. Hidaka, Fuel 87 (2007) 2798.
[25] Y.B. Cho, G. Seo, D.R. Chang, Fuel Process. Technol. 90 (2009) 1252.
[26] H. Lu, E.P. Reddy, P.G. Smirniotis, Ind. Eng. Chem. Res. 45 (2006) 3944.
[27] D. Tichit, B. Coq, H. Armendariz, F. Figuéras, Catal. Lett. 38 (1996) 109.
[28] C. Yang, J. Wang, Q. Xu, Micropor. Mater. 11 (1997) 261.
[29] O. Cairon, E. Dumitriu, C. Guimon, J. Phys. Chem. C 111 (2007) 8015.
[30] T.S. Yang, T.H. Chang, C.T. Yeh, J. Mol. Catal. A: Chem. 123 (1997) 163.
[31] H. Sun, Y. Ding, J. Duan, Q. Zhang, Z. Wang, H. Lou, X. Zheng, Bioresour. Technol. 101 (2010) 953.
[32] S. Liu, J. Ma, L. Guan, J. Li, W. Wei, Y. Sun, Micropor. Mesopor. Mater. 117 (2009) 466.
[33] R. Sree, N. Seshu Babu, P.S. Sai Prasad, N. Lingaiah, Fuel Process. Technol. 90 (2009) 152.
[34] M. Verziu, B. Cojocaru, J.C. Hu, R. Richards, C. Ciuculescu, P. Filip, V.I. Parvulescu, Green Chem. 10 (2008) 373.
[35] P. Liu, T. Kendelewicz, G.E.J. Brown, G.A. Parks, P. Pianetta, Surf. Sci. 416 (1998) 326.
[36] C.S. Doyle, T. Kendelewicz, X. Carrier, G.E. Brown, Surf. Rev. Lett. 6 (1999) 1247.